Available online at www.sciencedirect.com
SCIENCE DIRECT®
Journal of the European Ceramic Society 25 (2005) 1355–1358
www.elsevier.com/locate/jeurceramsoc

Continuous solidification of $YBa_2Cu_3O_{7-x}$ by isothermal undercooling

Fatih Dogan

University of Missouri-Rolla, Department of Materials Science and Engineering, 222 McNutt Hall, Rolla, MO 65409, USA

Available online 2 February 2005

Abstract

Growth kinetics and microstructural development of single crystal $YBa_2Cu_3O_{7-x}$ (Y123) superconductors, prepared by a melt texturing method under isothermal undercooling conditions, were investigated. At small undercooling, $\Delta T = 6$ K, the initial growth of Y123 crystal was terminated at a size of ~8 mm × 8 mm in the semisolid phase before the entire sample was fully solidified through the peritectic reaction. With incremental increase of ΔT, the growth of the crystal continued so that the whole sample (22 mm diameter and 8 mm thickness) solidified as a single crystal. Termination of the crystal growth at a given undercooling temperature was attributed to the coarsening process of Y211 particles in the melt associated with their surface energy contributions. Isothermal growth of large size Y123 single crystal requires a continuous supply of Y solute to the solidification interface which can be achieved by continuing dissolution of coarsening Y211 particles through further undercooling of the melt.

Keywords: Solidification; Inclusions; Microstructure-final; Oxide superconductors

1. Introduction

Melt textured $YBa_2Cu_3O_{7-x}$ (Y123) single crystals are utilized to achieve high critical current densities, J_c, for practical engineering applications of high temperature superconductors; such as superconducting bearings, flywheel systems for energy storage and fault current limiters.[1–3] Strong magnetic flux pinning capacity and high levitation forces are achieved by increasing the J_c and the loop size of the circulating current in Y123 single crystals. Hence, introducing of effective flux pinning sites for the enhancement of J_c, particularly in high magnetic fields, as well as enlargement of the crystal size are necessary for more demanding applications of high critical temperature, T_c, superconductors.

Several studies have been conducted to explain mechanisms and kinetic limitations for the growth of melt textured Y123 crystals from a semisolid melt consisting of Y211 solid phase dispersed in a liquid phase with a composition close to $3BaCuO_2$ and $2CuO$.[4–7] It is widely accepted that the peritectic reaction of 123 formation occurs by dissolution of Y211 particles in the melt, which, in turn, increases the Y-solute concentration in the liquid. The rate-limiting factor for the growth rate of Y123 is taken as the dissolution rate of Y211 phase which is controlled by the undercooling temperature and the size of Y211 inclusions. Melt textured Y123 single crystals were grown by continual cooling as well as constant undercooling methods to investigate the relationship between undercooling and growth rate.[4,8] The size and microstructural development of the crystals are controlled by the process parameters such as composition, temperature gradient, undercooling temperature, time, concentration of additives such as excess 211, Pt, etc. The size and concentration of the Y211 particles in the Y123 play an important role in enhancing of mechanical properties and flux pinning capacity of the crystals along with other imperfections such as twin boundaries, defects and nonsuperconducting inclusions.[9]

The engulfment and/or pushing of Y211 particles at the Y123-melt interface during the solidification process is

E-mail address: doganf@umr.edu.

0955-2219/$ – see front matter © 2005 Elsevier Ltd. All rights reserved.
doi:10.1016/j.jeurceramsoc.2005.01.009

explained qualitatively by the conventional particle pushing/trapping theory which was developed originally for the systems consisting of a melt composition with nonreactive particles in the liquid. Y211 particles in the liquid undergo a continuous change of the particle size through coarsening and dissolution processes which can significantly influence the growth rate, microstructural development and size of bulk crystals.[10–13] It is known that larger undercooling temperatures give rise to faster growth rates, which, in turn, leads to relatively larger crystal sizes, but may also result in polycrystalline samples due to increasing possibility of heterogeneous Y123 nucleation within the melt.

This study addresses solidification of Y123 crystals by seeded melt texturing method to understand the termination of crystal growth under isothermal undercooling conditions. Experimental parameters during solidification process, such as undercooling temperature and holding time, are discussed in the context of surface energy contributions of Y211 particles and continual growth of larger size single crystals.

2. Experimental procedure

Y123 powder containing 10 mol% excess Y211 phase and 0.2 wt.% Pt (Praxair Specialty Ceramics, Woodinville, WA) was used as starting material. A powder compact (∼30 mm in diameter and ∼10 mm thickness) was prepared by uniaxial pressing at a pressure of 200 MPa. A Sm123 single crystal, obtained by cleaving of a melt textured sample along the *a–b* plane, was used as a seed and placed on the top center of the powder compact with *c*-axis perpendicular to the surface of the sample.

For the melt textured growth process of Y123 single crystal, the pressed pellet was set on a barium zirconate setter and placed in a cold furnace under ambient air atmosphere. The sample was heated at a rate of 2 °C/min to 1050 °C above the peritectic decomposition temperature of ∼1010 °C and held for 1 h. Following the cooling at a rate of 1 °C/min, solidification of the sample took place by isothermal undercooling method at constant temperatures between 1004 and 990 °C with $\Delta T_1 = 6$ K, $\Delta T_2 = 12$ K and $\Delta T_3 = 20$ K. The holding times t_1, t_2 and t_3, corresponding to each undercooling temperature, were 7, 5 and 6 days, respectively (Fig. 1). During crystal growth, the sample was visually monitored in the furnace so that the growth rate of the crystals could be adjusted by decreasing the undercooling temperature incrementally. At ΔT_1, the growth of the crystal ceased after a holding time of 4 days and no noticeable growth was observed at prolonged holding times up to 3 days. However, further decrease of the undercooling temperature lead to continuation of the crystal growth process until the sample became completely a single crystal.

Distribution and size of Y211 particles as well as other surface futures on the crystal were observed by scanning electron microscopy (SEM JOEL-T330A) techniques equipped with electron dispersive spectrometer (EDS) for compositional analysis. The liquid loss was determined by the weight difference of the sample before and after the solidification process.

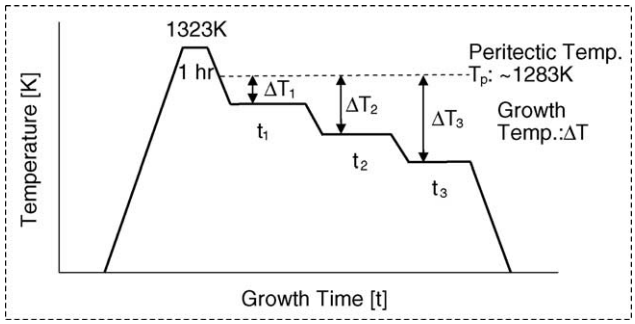

Fig. 1. Temperature and time profile during solidification process of Y123.

3. Results and discussion

The top view of a melt textured Y123 single crystal (22 mm diameter, 8 mm thickness) with a Sm123 seed in the center is depicted in Fig. 2. Solidification of the sample was initiated at the seed crystal epitaxially without any multiple nucleation problems. Two distinct square facets on the surface indicate the locations of the solid–melt interface at which the crystal growth was terminated after prolonged holding times at undercooling temperatures ΔT_1 and ΔT_2. The entire sample solidified as a single crystal at ΔT_3 and after holding time t_3. Growth sector boundaries along the *a–b* plane (1 0 0) are noticeable inside the first square as diagonal lines starting at the seed. Fig. 3 shows a schematic diagram of the sample and the locations, from which the SEM images were taken.

Melt processing of Pt-doped Y123 samples results in the formation of platelet-like $Ba_4CuPt_2O_9$ particles which form aggregates in the liquid phase through particle clustering. The size of the clusters increases with time resulting in rougher

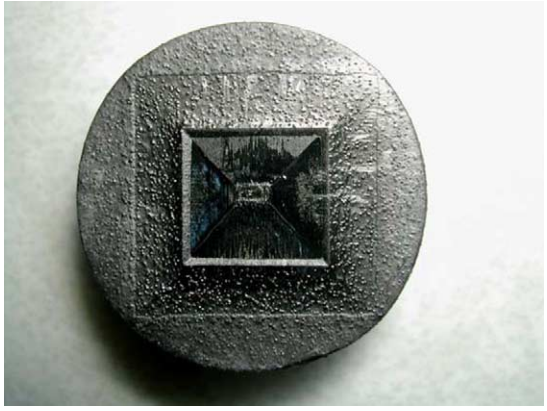

Fig. 2. Melt textured Y123 single crystal (22 mm diameter, 8 mm thickness) showing interfaces caused by termination/continuation of solidification at different undercooling temperatures.

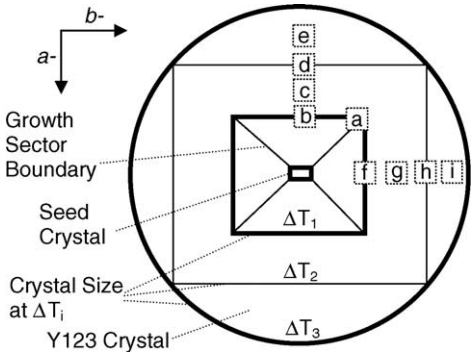

Fig. 3. Schematic diagram of the crystal indicating locations for microstructural characterization.

surface of the crystal after the initial growth process (Fig. 2). The aggregation process indicates a poor wetting behavior of $Ba_4CuPt_2O_9$ platelets by the liquid phase as shown in Fig. 4.

Fig. 5a reveals the microstructure of the sample at the location "a" and the growth sector boundary (GSB) as a diagonal line. While the growth sector on the left side of the GSB is free of Y211 particles, the sector on the right side of the GSB reveals entrapped Y211 particles. The faceted interface indicates termination of the crystal growth at undercooling temperature ΔT_1. Solute composition measurements of quenched samples, conducted by Hanjo et al., show that there is a significant difference in the composition of the liquid ahead of each growing face.[14] The copper oxide content in the liquid was found to be lower at the (0 0 1) interface compared with (1 0 0) or (0 1 0) interfaces. It was suggested that this difference in the solute composition acts as the driving force for Y211 particle segregation. This was explained by the large diffusion length of solute and the low growth rate may allow significant mass transport in the liquid leading to different concentration of Y211 particles along the axis of Y123. Analogously, the differences in Y211 volume fractions along the *a*- and *b*-axes in Fig. 5a may be attributed to the similar phenomena during the initial stage of crystal growth at ΔT_1. Furthermore, the particle pushing phenomena appears also to contribute to the higher Y211 particle concentration at the interface along the *a*-axes (Fig. 5b) than that at the interface along the *b*-axes (Fig. 5f). Coarsening of Y211 particles in the melt at the later stages of crystal growth (t_2 and t_3) results in slower dissolution of larger Y211 particles so that the population density of Y211 remain similar along both axis of the crystal.

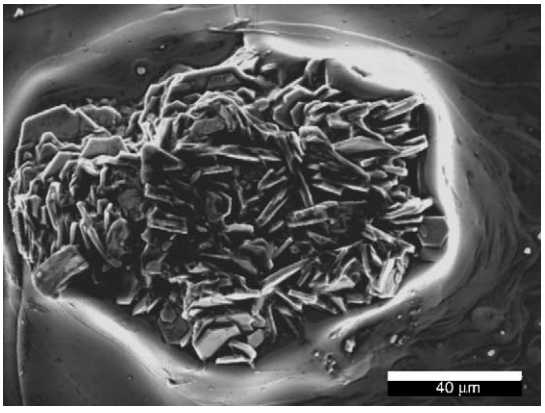

Fig. 4. Clustered of $Ba_4CuPt_2O_9$ platelets forming large size aggregates.

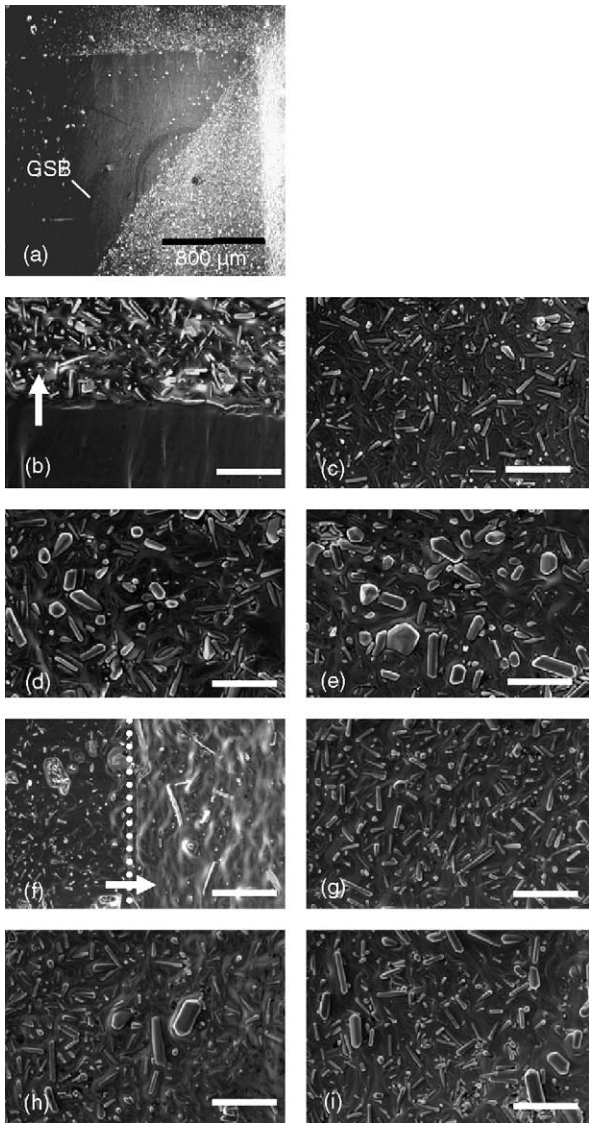

Fig. 5. Microstructural development on the surface of the crystal showing the interface and Y211 particles at different locations (a–i) as depicted in Fig. 3. Size bar: 40 μm.

Non-steady-state solidification of Y123 under isothermal undercooling conditions was also observed by Kambara et al.[15] A sudden decrease in crystal growth rate was found for Y123 samples processed at different temperatures. Termination of the crystal growth was explained by pushing/entrapping behavior of Y211 particles accumulating in the liquid ahead of the growth interface. It was further concluded that in the process of accumulation, the particles decrease the connectivity of the liquid and thereby inhibit the liquid diffusion, which eventually causes the termination of

solidification.[15,16] However, Figs. 1 and 5b and f indicate that termination of the crystal growth is not affected by the population density of Y211 at the solidification front. Although relatively low concentration of Y211 particles are present at the interface "f" (Fig. 5f) in comparison to the interface "b" (Fig. 5b), the size of the growing crystal in both crystallographic directions remain the same. Similarly, no particle accumulation is observed along the interfaces "d" and "h" so that the termination of solidification cannot be attributed to inhibition of the liquid diffusion by Y211 particles.

Particle size influences both the thermodynamics and kinetics of dissolution and precipitation reactions.[17] These effects are due to the contribution of the surface energy to the free energy of the solid phase. Owing to their large surface to volume ratios, and hence their large surface (interfacial) free energies, small particles (<1 μm) are inherently less stable than large particles.[4,9] Y211 particles with greater total surface free energy coarsen with time by Ostwald ripening mechanism according to the equation:

$$r^3 - r_0^3 = at$$

where $r_0 < 0.05\,\mu m$, $a = 8.1 \times 10^{-21}\,m^3/s$, and t is time.[4,14] This relationship indicates a rapid initial growth of particles in the melt within a relatively short period of time (coarsening from 0.05 to 0.5 μm in ∼3 min). Ostwald ripening results also in broadening of particle size distribution and a decrease in the number of particles. Hence, during the initial stage of solidification, a relatively fast dissolution of smaller Y211 particles takes place at a small undercooling (ΔT_1) which, in turn, corresponds to a higher solidification rate of Y123.[18] Rapid dissolution of Y211 phase is attributed to the higher surface free energy of fine particles. As the coarsening of particles proceeds, a sluggish dissolution reaction of Y211 results in a slower growth of Y123 crystal. Therefore, the rate-limiting factor for solidification of Y123 is the total surface area (or surface energy) of particles affecting the dissolution rate of Y211 phase. The increase of the particle size is expected to produce continuous energy changes over a temperature range of undercooling. Fig. 5b–i shows coarsening of Y211 particles as a function of time and undercooling temperature. Solidification is terminated at each undercooling temperature after a certain time at which Y211 particles exceed a threshold size by Ostwald ripening. Hence, Y211 particles larger than a critical size do not supply a sufficient amount of solute for solidification of Y123 phase at a constant ΔT, while the dissolution–precipitation process favors coarsening of Y211 particles. Through further undercooling, the system returns to the thermodynamically favorable state by reinitiating the solidification process but with a relatively slow rate controlled by slow dissolution rate of coarser Y211 particles.

4. Summary

The undercooling temperature and surface energy contributions of Y211 particles in the melt play a key role inthe isothermal solidification of Y123 single crystals by melt texturing process. Termination of solidification occurs due to coarsening of Y123 particles which limits the Y-solute supply into the liquid by dissolution process. Solidification of Y123 crystal continues by lowering the undercooling temperature (increasing ΔT) of the melt which, in turn, leads to increased dissolution rate of coarse Y211 particles.

References

1. Jin, S., Tiefel, T. H., Sherwood, R. C., van Dover, R. B., Davis, M. E., Kammlott, G. W. *et al.*, *Phys. Rev. B*, 1988, **37**, 7850.
2. Murakami, M., Morita, M., Doi, K. and Miyamoto, K., *Jpn. J. Appl. Phys.*, 1989, **28**, 1189.
3. Fujimoto, H., Murakami, M., Gotoh, S., Koshizuka, N., Oyama, T., Shiohara, Y. *et al.*, *Adv. Supercond.*, 1990, **II**, 285.
4. Cima, M. J., Flemings, M. C., Figueredo, A. M., Nakade, M., Isii, H., Brody, D. *et al.*, *J. Appl. Phys.*, 1992, **72**, 179.
5. Izumi, T. and Shiohara, Y., *J. Mater. Res.*, 1992, **7**, 16.
6. Bateman, C. A., Zhang, L., Chan, H. M. and Harmer, M. P., *J. Am. Ceram. Soc.*, 1992, **75**, 281.
7. Goyal, A., Alexander, K. B., Kroeger, D. M., Funkenbush, P. D. and Burns, S. J., *Physica C*, 1993, **210**, 197.
8. Endo, A., Chauhan, H. S., Egi, T. and Shiohara, Y., *J. Mater. Res.*, 1996, **11**, 795.
9. Shiohara, Y. and Endo, A., *Mater. Sci. Eng., R*, 1997, **19**, 1.
10. Varanasi, C. and McGinn, P. J., *Physica C*, 1993, **207**, 79.
11. Kim, C. J., Kim, K.-B., Hong, G.-W. and Lee, H.-Y., *J. Mater. Res.*, 1995, **10**, 1605.
12. Sakai, N., Yoo, S. I. and Murakami, M., *J. Mater. Res.*, 1995, **10**, 1611.
13. Varanasi, C., Black, M. A. and McGinn, P. J., *J. Mater. Res.*, 1996, **11**, 565.
14. Hanjo, S., Cima, M. J., Flemings, M. C., Ohkuma, T., Shen, H., Rigby, K. *et al.*, *J. Mater. Res.*, 1997, **12**, 880.
15. Kambara, M., Yoshizumi, M., Umeda, T., Miyake, K., Murata, K., Izumi, T. *et al.*, *J. Mater. Res.*, 2001, **16**, 2229.
16. Nakamura, Y., Kambara, M., Izumi, T. and Shiohara, Y., *Physica C*, 2000, **341–348**, 2417.
17. Morel, F. M. M. and Hering, J. G., *Principles and Applications of Aquatic Chemistry*. John Wiley & Sons, New York, 1993, pp. 300–301.
18. Dogan, F. and Reding, J. D., Impact of recent advances in processing of ceramic superconductors. In *Ceramic Transactions, Vol 84*, ed. U. Balachandran, W. Wong-Ng and A. Bhalla. American Ceramic Society, Westerville, OH, 1998, pp. 23–30.